Journal of Organometallic Chemistry, 436 (1992) 127–142
Elsevier Sequoia S.A., Lausanne
JOM 22778

Molecular geometry and ring deformation of trimethylsilylbenzenes: gas-phase electron-diffraction study of 1,3-bis(trimethylsilyl)benzene and 1,3,5-tris(trimethylsilyl)benzene

Béla Rozsondai [a] and István Hargittai [a,b]

[a] *Structural Chemistry Research Group of the Hungarian Academy of Sciences, Eötvös University, P.O. Box 117, H-1431 Budapest (Hungary)*
[b] *Institute for General and Analytical Chemistry, Technical University of Budapest, H-1521 Budapest (Hungary)*

(Received January 16, 1992)

Abstract

The molecular geometries of 1,3-$C_6H_4(SiMe_3)_2$ (**2**) and 1,3,5,-$C_6H_3(SiMe_3)_3$ (**3**) have been determined by gas-phase electron diffraction. The mean C–C bond lengths are slightly larger than those in benzene, and the endocyclic *ipso* bond angles C6–C1–C2 are considerably less than 120°, in accord with the electron-releasing inductive effect of the $SiMe_3$ substituent and the predictions of the VSEPR model. The Si–C (methyl) bonds are longer than the Si–C(aryl) bonds by about 0.02 Å (see below). Only limited information concerning conformational preference could be obtained from the electron-diffraction data but this did not hinder the determination of the other structural characteristics. The following main bond length (r_g) and angle parameters (with estimated total errors) have been obtained at nozzle temperatures of 86 and 105°C, respectively. For **2**: $(C–C)_{mean}$ 1.405 ± 0.003, $(Si–C)_{mean}$ 1.879 ± 0.004, $\Delta(SiC)$ = Si–C(methyl) – Si–C(aryl) = 0.018 ± 0.008, Si–C(methyl) 1.884 ± 0.004, Si–C(aryl) 1.866 ± 0.007 Å, C6–C1–C2 116.2 ± 0.6°, C4–C5–C6 119.5° (assumed), C–Si–C 109.5° (assumed); for **3**: C–C 1.410 ± 0.003, $(Si–C)_{mean}$ 1.881 ± 0.004, $\Delta(SiC)$ 0.016 ± 0.006, Si–C(methyl) 1.885 ± 0.004, Si–C(aryl) 1.869 ± 0.006 Å, C6–C1–C2 117.0 ± 0.6°, C–Si–C 109.5° (assumed). On the basis of available structural information on three trimethylsilyl-substituted benzene derivatives, and assuming additivity, the angular ring deformation impact of the trimethylsilyl substituent has been estimated. The predicted endocyclic angles for trimethylsilylbenzene are (starting from the *ipso* angle) 116.8, 122.2, 119.9, and 119.0°.

Introduction

Substituent effects on benzene ring geometry have been extensively studied in both the gas and crystalline phases, and correlations with other properties of the substituents have been observed [1]. A distortion of the benzene ring was first noted in the electron-diffraction study of phenylsilane [2], and yet, only a small

---

Correspondence to: Dr. B. Rozsondai.

number of aryl silanes has been subjected to gas-phase structural study [3–6] and little or no information on the distortion of the aromatic ring has been obtained. The characteristic deformation caused by a silyl substituent was deduced from X-ray crystallographic data [7].

Some years ago we determined the structure of 1,4-bis(trimethylsilyl)benzene (**1**) [4]. Now, at Professor T. Sonoda's suggestion (arising from his studies of the effects of Me_3Si groups on the stability of aryl cations [8,9]), we have returned to study of trimethylsilylbenzenes by gas-phase electron diffraction. These structures pose three main questions: the extent of distortion of the benzene ring, the values of the bond lengths and angles at silicon, and the conformational properties, which can be only partly answered from electron diffraction data alone. We report here the structures of 1,3-bis(trimethylsilyl)benzene (**2**) and 1,3,5-tris(trimethylsilyl)benzene (**3**). Preliminary results have been communicated [10].

Analysis

Samples of **2** and **3** were provided by Professor Sonoda, who prepared them from the corresponding bromobenzenes [11], purified them by vacuum distillation, and used a Shimadzu GC 14 gas chromatograph to show the purities to be 99.69 and 99.74%, respectively. A check some months later, immediately before the diffraction experiments, gave the same results.

Electron diffraction patterns were recorded in a modified EG-100A apparatus [12] with a membrane nozzle [13] at 60 kV nominal accelerating voltage. We followed our usual procedures of data reduction, structure analysis, and error estimation [5,6,14]. Smooth background lines were obtained and corrected by fitting polynomials, with occasional manual graphical adjustments. Mean nozzle temperatures, the numbers of photographic plates evaluated from the two camera distances, and data ranges of reduced molecular intensities [14] were as follows. 1,3,-bis(trimethylsilyl)benzene (**2**), 86°C: 50 cm, 8 plates, $1.875 \leq s \leq 14.000$, $\Delta s = 0.125$ Å^{-1}; 19 cm, 7 plates, $9.250 \leq s \leq 36.000$, $\Delta s = 0.250$ Å^{-1}. 1,3,5-tris(trimethylsilyl)benzene (**3**), 105°C: 50 cm, 8 plates, $1.875 \leq s \leq 14.125$, $\Delta s = 0.125$ Å^{-1}; 19 cm, 6 plates, $9.250 \leq s \leq 36.000$, $\Delta s = 0.250$ Å^{-1}.

Final molecular intensities and difference curves are plotted in Figs. 1 and 2.

Molecular parameters were refined, based on molecular intensities with unit weights, by a least-squares program [15] modified and adapted for use on a personal computer. Coherent and incoherent scattering factors were interpolated from tabulated values [16].

As expected, the radial distribution curves for the two molecules look very similar (Figs. 3 and 4) and, consequently similar problems arise in their analyses. The mean bond lengths, C–H, C–C, and Si–C are each well defined from the first three peaks. Overlapping contributions of nonbonded distances at 2.4 and 2.8–3.1 Å make the determination of bond angles difficult, and result in strong correlations between angles, bond length differences, and vibrational amplitudes. Si ··· C and Si ··· Si distances which are independent of the conformation dominate the peaks at 4.2, 4.7, and 5.7 Å. Conformation-dependent ring-carbon to methyl-carbon internuclear distances span the range from 3.3–5.5 Å, but their overall contribution is much the same in all possible conformers. More characteristic of the

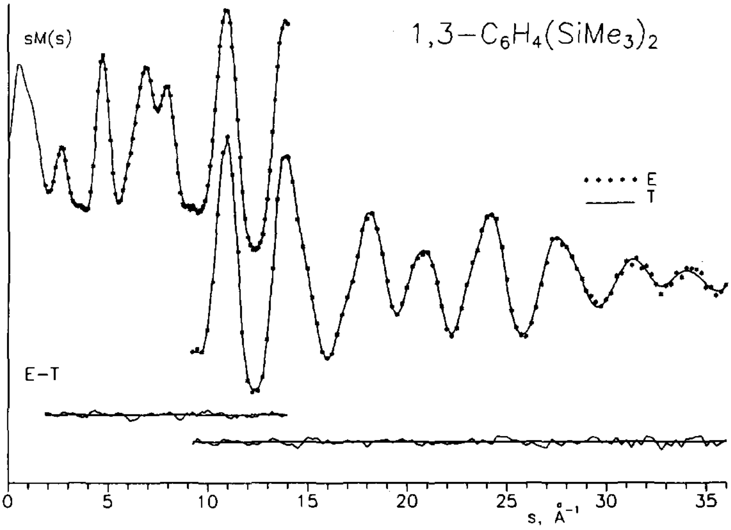

Fig. 1. Experimental (E) and calculated (T) molecular intensities of **2** and the difference curves (E − T) for the model in Table 1.

conformation are the silicon to methyl carbon distances of > 5.6 Å, and the smaller contributions from the methyl C ··· C distances in about the same range.

The geometry of molecular models was defined by the independent parameters listed in Tables 1 and 2. The following symmetry properties of models were assumed: C_{2v} point group symmetry for the $C_6H_4Si_2$ moiety, with the C–Si and C–H bonds bisecting the exocyclic angles; D_{3h} for the $C_6H_3Si_3$ moiety; local C_{3v} symmetry of the C–SiMe$_3$ and Si–CH$_3$ fragments with staggered methyl groups.

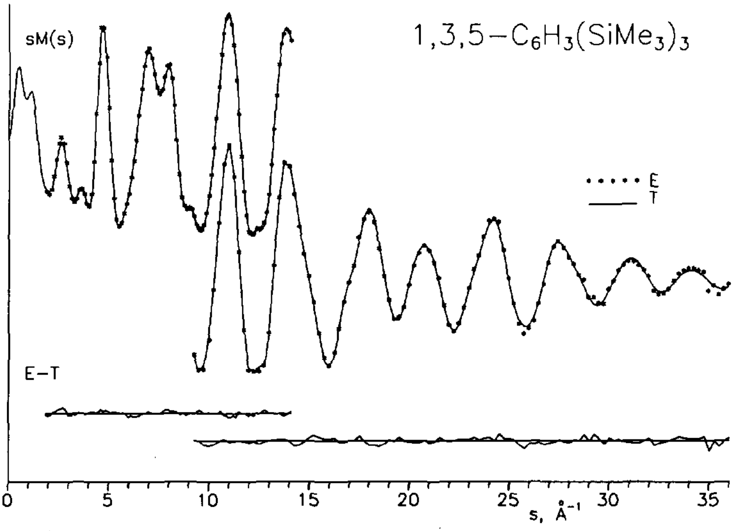

Fig. 2. Experimental (E) and calculated (T) molecular intensities of **3** and the difference curves (E − T) for the model in Table 2.

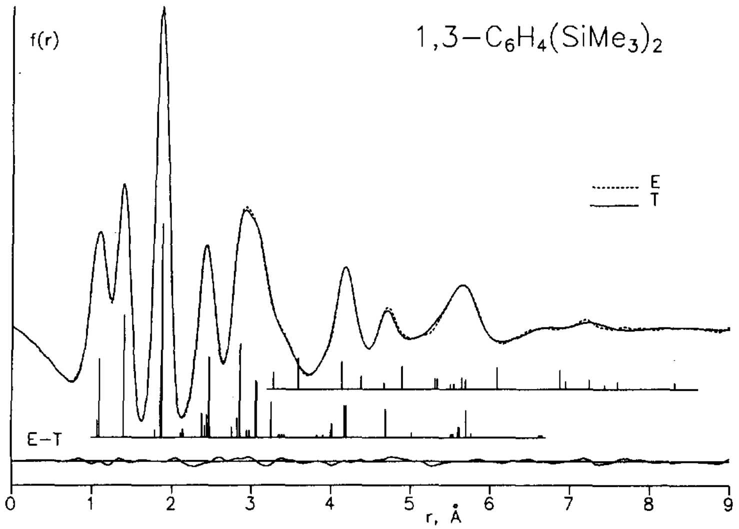

Fig. 3. Experimental (E) and calculated (T) radial distribution of **2** and the difference curve (E − T) for the model in Table 1. Damping constant $a = 0.002$ Å^2. Rotation-dependent Si···C and C···C contributions are shown separately.

Conformation was specified, using the IUPAC sign convention [17], by torsional angles τ_1(C2–C1–Si1–C11), τ_3(C4–C3–Si3–C31), and, for the trisubstituted derivative, τ_5(C6–C5–Si5–C51) in addition (Fig. 5). Thus, for example, if $\tau_1 = 0$ or 180°, the Si1–C11 bond lies in the ring plane. The range 0° ≤ τ_1 ≤ 30° describes all

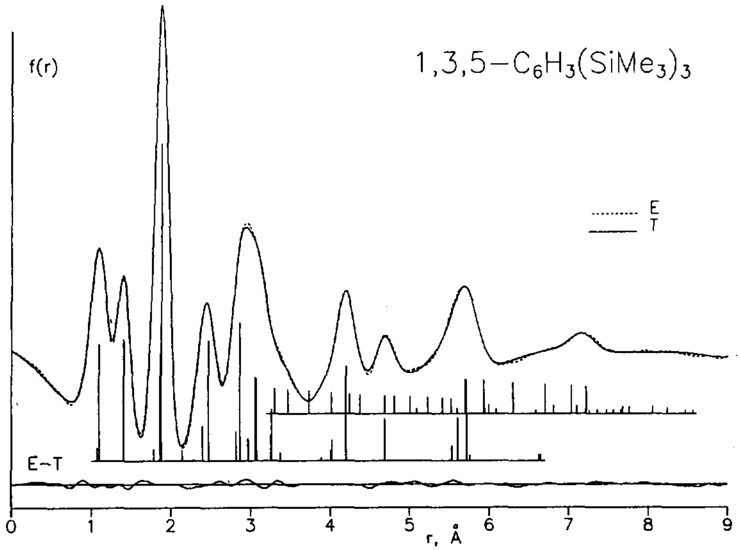

Fig. 4. Experimental (E) and calculated (T) radial distribution of **3** and the difference curve (E − T) for the model in Table 2. Damping constant $a = 0.002$ Å^2. Rotation-dependent Si···C and C···C contributions are shown separately.

possible relative positions of the benzene ring and a single $SiMe_3$ substituent. Additional ranges are needed to generate models with different mutual positions of the $SiMe_3$ groups in the di- and trisubstituted derivatives. We confined the structure analysis of **2** to models in which the two $SiMe_3$ groups are rotated by the same angle τ_i' (regarding the absolute values) from a 'coplanar' $\tau_i = 0°$ or 180° position. Thus, $\tau_3' = \tau_1'$ for these models [18*]. Two kinds of models were involved in the analysis of **3**: (1) models with $\tau_5' = \tau_3' = \tau_1'$ and (2) models of C_s symmetry with $\tau_5' = \tau_1'$ and $\tau_3 = 90°$. All models complying with the above restrictions are represented in Figs. 6 and 7.

Initial values of parameters were estimated from the data for related molecules; *e.g.* from the calculated vibrational amplitudes of **1** [4]. Some of the parameters had eventually to be fixed at assumed values (see Tables 1 and 2) because of unrealistic refined values, poor convergence, or high correlations. Amplitudes were refined in 14 to 18 groups corresponding to ranges of the radial distribution, those for the longer $C \cdots H$ interactions were kept fixed throughout. Many different initial parameter sets and refinement schemes were tried.

Discussion

The results of the structure analysis of **2** and **3** are presented in Tables 1 and 2, and selected elements of the correlation matrices from the same refinements are listed in Tables 3 and 4. Important geometrical parameters are summarized and compared with those of **1**, in Table 5. Even though some of them are badly correlated with others, the parameters in Table 5 had only small variations in the 'acceptable' models. For **2** and **3** in Tables 1, 2, and 5, the total estimated error of a parameter includes the least-squares standard deviation with effects of experimental data correlation, a systematic (scale) error [14], and an additional term which should account for some of the restrictions and was chosen as the largest variation of this parameter in refinements of the best assumed conformers (see below). Forms that agreed poorly with the experimental data were disregarded in the error estimation since the strong discrepancies in the conformation-dependent contributions may bias other contributions as well.

Ring geometry

The mean C–C bond lengths are well determined from the electron-diffraction data (Table 5). They are slightly larger than the value of r_g, 1.399 ± 0.001 Å, reported for benzene [19]. In **1**, the bond C1–C2 adjacent to the substituent is longer by 0.016 ± 0.007 Å than the central bond C2–C3 [4]. The *ipso* bond angles C6–C1–C2 in the three molecules are considerably smaller than 120°. These bond length and bond angle changes from the unsubstituted benzene ring are consistent with the VSEPR model [20] and with expectations for the electron-releasing trimethylsilyl substituent [1]. The ring geometries in **1** (D_{2h} symmetry) and in **3** (D_{3h}) are completely defined by the parameters above. The remaining parameters had to be assumed for the C_{2v} ring of **2**, and the individual C–C bond lengths could not be obtained (Table 1). Use of good *ab initio* quantum chemical data in

---

* Reference number with asterisk indicates a note in the list of references.

Table 1

Refined structural parameters of **2** [a]

	r_a, ∠ with least-squares standard deviations (Å, deg.)	l (Å)	l group no.	r_g, ∠ with estimated total errors (Å, deg.)
Independent parameters [b]				
(C–C)$_{mean}$	1.4037(5)			1.405 ± 0.003
Δ_1(CC)	0.0 [c]			
Δ_6(CC)	0.0 [c]			
(Si–C)$_{mean}$	1.8776(3)			1.879 ± 0.004
Δ(SiC)	0.018(5)			0.018 ± 0.008
(C–H)$_{mean}$	1.093(1)			1.099 ± 0.005 [d]
Δ(CH)	0.025 [c]			
C6–C1–C2	116.2(4)			116.2 ± 0.6
C4–C5–C6	119.5 [c]			
θ	0.0 [c]			
C1–Si–C11	109.5 [c]			
Si–C–H	109.5 [c]			
τ_1	0.0 [c]			
Dependent parameters, nonbonded distances				
τ_3	0.0 [c]			
C1–C2–C3	125.0(6)			125.0 ± 0.9
C3–C4–C5	121.6(1)			121.6 ± 0.2
C2–C1–Si1	121.9(2)			121.9 ± 0.3
C1–C2	1.4037(5)	0.0494(7)	1	1.405 ± 0.003
Si1–C1	1.864(4)	0.0548(6)	2	1.866 ± 0.007
Si1–C11	1.882(1)	0.0568	2	1.884 ± 0.004
C2–H2	1.073(1)	0.085(1)	3	
C11–H111	1.098(1)	0.086	3	
C1 ··· C3	2.490(6)	0.055(3)	4	
C1 ··· C5	2.450(2)	0.055	4	
C2 ··· C4	2.384(6)	0.055	4	
C4 ··· C6	2.425(1)	0.055	4	
C1 ··· C4	2.830(3)	0.071(2)	5	
C2 ··· C5	2.759(7)	0.072	5	
C1 ··· C11	3.059(2)	0.113(2)	6	
C11 ··· C12	3.073(2)	0.106	6	
C4 ··· C11	5.597(2)	0.199(6)	7	
C4 ··· C12	5.617(1)	0.199	7	
C6 ··· C31	5.623(2)	0.199	7	
C6 ··· C32	5.603(2)	0.199	7	
Si ··· Si	5.699(3)	0.119	7	
Si1 ··· C2	2.865(1)	0.083	5	
Si1 ··· C3	4.203(3)	0.079(2)	8	
Si1 ··· C5	4.180(2)	0.079	8	
Si1 ··· C4	4.694(2)	0.076(4)	9	
Si1 ··· H111	2.475(1)	0.125	4	
Si1 ··· H2	2.953(3)	0.144	6	
Si1 ··· H6	2.983(2)	0.144	6	
Si1 ··· H5	5.019(2)	0.122(17)	10	
Si1 ··· H4	5.766(2)	0.156	7	
C1 ··· H2	2.124(4)	0.095(9)	11	
C1 ··· H6	2.143(2)	0.095	11	
C4 ··· H5	2.154(1)	0.095	11	

Table 1 (continued)

	r_a, ∠ with least-squares standard deviations (Å, deg.)	l (Å)	l group no.	r_g, ∠ with estimated total errors (Å, deg.)
C5 ··· H4	2.143(2)	0.095	11	
C1 ··· H5	3.418(2)	0.110(6)	12	
C2 ··· H4	3.363(5)	0.110	12	
C4 ··· H2	3.352(6)	0.110	12	
C4 ··· H6	3.393(2)	0.110	12	
C1 ··· H4	3.903(3)	0.082(10)	13	
C2 ··· H5	3.832(7)	0.082	13	
C1 ··· H111	4.004(3)	0.121	13	
C1 ··· H112	3.253(2)	0.237	12	
C4 ··· H111	6.641[c]	0.161[c]		
C4 ··· H121	6.655[c]	0.161[c]		
C4 ··· H112	5.511[c]	0.302[c]		
C4 ··· H122	5.526[c]	0.302[c]		
C4 ··· H123	5.540[c]	0.302[c]		
C11 ··· H4	6.617[c]	0.180[c]		
C12 ··· H4	6.631[c]	0.180[c]		
C11 ··· H121	3.263(2)	0.242	12	
C11 ··· H123	4.020(2)	0.118	13	
H111 ··· H112	1.792(2)	0.129[c]		
C1 ··· C31	5.544(4)	0.159	7	
C1 ··· C32	4.898(2)	0.182	10	
C2 ··· C11	3.286(2)	0.172	12	
C2 ··· C12	4.140(1)	0.178	8	
C2 ··· C31	4.388(1)	0.109	8	
C2 ··· C32	3.593(2)	0.175(13)	14	
C3 ··· C11	4.663(1)	0.175	9	
C3 ··· C12	5.338(4)	0.176	10	
C5 ··· C11	5.501(2)	0.159	7	
C5 ··· C12	4.895(2)	0.182	10	
C5 ··· C31	4.675(2)	0.175	9	
C5 ··· C32	5.306(1)	0.176	10	
C11 ··· C31	7.437(3)	0.200(27)	15	
C11 ··· C32	5.692(6)	0.241	7	
C12 ··· C31	8.314(3)	0.397[c]		
C12 ··· C32	6.951(3)	0.305(33)	16	
C12 ··· C33	7.600(2)	0.417[c]		
Si1 ··· C31	7.244(2)	0.160	15	
Si1 ··· C32	6.086(4)	0.272(42)	17	
Si3 ··· C11	5.648(5)	0.211	7	
Si3 ··· C12	6.880(2)	0.285	16	
R	0.046			

---

[a] Least-squares standard deviations in parentheses are in units of the last digit, and are given only once for a group of amplitudes (l). See text for the estimation of total errors. Conformation-dependent Si ··· H and C ··· H distances are not listed. [b] $\Delta_1(\mathrm{CC}) = r(\mathrm{C1{-}C2}) - r(\mathrm{C6{-}C1})$, $\Delta_6(\mathrm{CC}) = r(\mathrm{C6{-}C1}) - r(\mathrm{C5{-}C6})$, $\Delta(\mathrm{SiC}) = r(\mathrm{Si1{-}C11}) - r(\mathrm{Si1{-}C1})$, $\Delta(\mathrm{CH}) = r(\mathrm{C11{-}H111}) - r(\mathrm{C2{-}H2})$, θ is the tilt of the Si1–C1 bond from the exocyclic bisector of angle C6–C1–C2: $2\theta = \angle(\mathrm{C2{-}C1{-}Si1}) - \angle(\mathrm{C6{-}C1{-}Si1})$, τ_1 is the dihedral angle C2–C1–Si1–C11, *etc.* (Fig. 5). [c] Fixed parameter. [d] Considering the discrepancy between the refined l(C–H) in **2** and **3**, we used l(C–H) = 0.078 Å to convert r_a to r_g: $r_g = r_a + l^2/r_a$, and increased the error estimate of r_g(C–H) by 0.002 Å.

Table 2

Refined structural parameters of **3** [a]

	r_a, ∠ with least-squares standard deviations (Å, deg.)	l (Å)	l group no.	r_g, ∠ with estimated total errors (Å, deg.)
Independent parameters [b]				
C–C	1.4082(8)	0.0515(10)	1	1.410 ± 0.003
(Si–C)$_{\mathrm{mean}}$	1.8793(3)			1.881 ± 0.004
Δ(SiC)	0.016(4)			0.016 ± 0.006
(C–H)$_{\mathrm{mean}}$	1.094(1)			1.099 ± 0.005 [d]
Δ(CH)	0.025 [c]			
C6–C1–C2	117.0(4)			117.0 ± 0.6
C1–Si–C11	109.5 [c]			
Si–C–H	109.5 [c]			
τ_1	165.0 [c]			
Dependent parameters, nonbonded distances				
τ_3	−15.0 [c]			
τ_5	15.0 [c]			
C1–C2–C3	123.0(4)			123.0 ± 0.6
Si1–C1	1.867(3)	0.0552(5)	2	1.869 ± 0.006
Si1–C11	1.883(1)	0.0572	2	1.885 ± 0.004
C2–H2	1.071(1)	0.075(1)	3	
C11–H111	1.096(1)	0.076	3	
C1 ··· C3	2.475(4)	0.061(2)	4	
C2 ··· C4	2.401(5)	0.061	4	
C1 ··· C4	2.816(2)	0.075(2)	5	
C1 ··· C11	3.063(2)	0.118(2)	6	
C11 ··· C12	3.075(2)	0.111	6	
C2 ··· C51	5.600(3)	0.207(3)	7	
Si ··· Si	5.709(2)	0.127	7	
Si1 ··· C2	2.867(1)	0.087	5	
Si1 ··· C3	4.198(2)	0.081(2)	8	
Si1 ··· C4	4.683(3)	0.080(4)	9	
Si1 ··· H111	2.476(1)	0.131	4	
Si1 ··· H2	2.967(1)	0.149	6	
Si1 ··· H4	5.754(4)	0.164	7	
C1 ··· H2	2.138(3)	0.099(18)	10	
C2 ··· H4	3.372(5)	0.135(6)	11	
C1 ··· H4	3.887(2)	0.091(8)	12	
C1 ··· H111	4.007(2)	0.130	12	
C1 ··· H112	3.256(1)	0.262	11	
C2 ··· H511	6.649(3)	0.212(19)	13	
C2 ··· H512	5.525(2)	0.351	7	
C11 ··· H4	6.625(3)	0.231	13	
C11 ··· H121	3.265(2)	0.267	11	
C11 ··· H123	4.021(2)	0.127	12	
H111 ··· H112	1.790(2)	0.129 [c]		
C1 ··· C31	5.519(3)	0.173	7	
C1 ··· C32	5.007(2)	0.267(26)	14	
C1 ··· C33	4.807(2)	0.186	9	
C1 ··· C51	4.687(2)	0.180	9	
C1 ··· C52	5.415(3)	0.207	7	
C1 ··· C53	5.230(2)	0.267	14	
C2 ··· C11	4.377(1)	0.117	8	

Table 2 (continued)

	r_a, ∠ with least-squares standard deviations (Å, deg.)	l (Å)	l group no.	r_g, ∠ with estimated total errors (Å, deg.)
C2 ··· C12	3.733(2)	0.187	12	
C2 ··· C13	3.468(2)	0.125(11)	15	
C4 ··· C31	3.305(2)	0.199	11	
C4 ··· C32	4.018(1)	0.183	12	
C4 ··· C33	4.249(1)	0.158	8	
C11 ··· C31	8.563(2)	0.189(37)	16	
C11 ··· C32	7.763(2)	0.209	16	
C11 ··· C33	7.678(2)	0.209	16	
C11 ··· C51	5.084(3)	0.280	14	
C11 ··· C52	7.099(2)	0.177(11)	17	
C11 ··· C53	6.808(2)	0.211	13	
C12 ··· C32	7.207(2)	0.187	17	
C12 ··· C33	5.998(2)	0.294(25)	18	
C12 ··· C52	8.241(2)	0.219	16	
C12 ··· C53	7.258(2)	0.187	17	
C13 ··· C33	6.085(2)	0.294	18	
C13 ··· C52	8.054(2)	0.219	16	
C31 ··· C51	7.476(2)	0.167	17	
C31 ··· C52	5.597(2)	0.209	7	
C31 ··· C53	5.948(2)	0.284	18	
C32 ··· C51	8.059(2)	0.209	16	
C32 ··· C52	6.587(2)	0.221	13	
C32 ··· C53	7.656(2)	0.219	16	
C33 ··· C51	8.469(2)	0.209	16	
C33 ··· C52	7.566(2)	0.219	16	
C33 ··· C53	7.362(2)	0.187	17	
Si1 ··· C31	7.222(2)	0.137	17	
Si1 ··· C32	6.304(2)	0.201	13	
Si1 ··· C33	5.933(2)	0.274	18	
Si1 ··· C51	5.707(2)	0.209	7	
Si1 ··· C52	7.038(2)	0.157	17	
Si1 ··· C53	6.707(2)	0.191	13	
R	0.044			

---

[a] Least-squares standard deviations in parentheses are in units of the last digit, and are given only once for a group of amplitudes (l). See text for the estimation of total errors. Conformation-dependent Si ··· H and C ··· H distances are not listed. [b] Δ(SiC) = r(Si1–C11) – r(Si1–C1), Δ(CH) = r(C11 ··· H111) – r(C2–H2), τ_1 is the dihedral angle C2–C1–Si1–C11, *etc.* (Fig. 5). [c] Fixed parameter. [d] Considering the discrepancy between the refined l(C–H) in **2** and **3**, we used l(C–H) = 0.078 Å to convert r_a to r_g: $r_g = r_a + l^2/r_a$, and increased the error estimate of r_g(C–H) by 0.002 Å.

the electron-diffraction analysis, primarily for the small bond length differences, would help to determine other parameters more reliably.

Statistical analyses of mainly X-ray crystallographic data have shown additivity of the angular deformations of the benzene ring in multisubstituted derivatives unless special effects are operating [1]. Angular deformation components for various substituents have been derived [21], but there were no such data for the trimethylsilyl substituent. We have attempted a rough prediction of the ring angular deformation parameters from the experimental data now available for

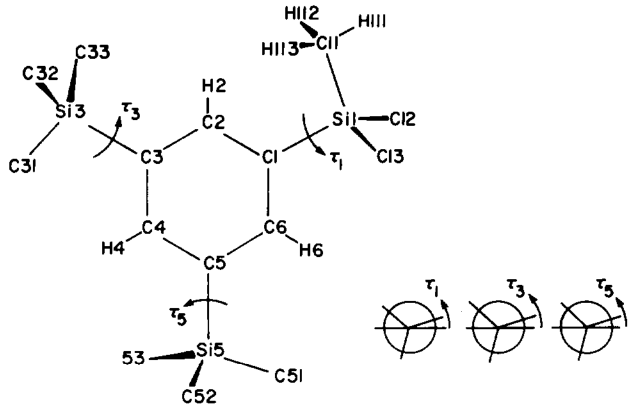

Fig. 5. Numbering of atoms in **3**, with some of the hydrogen atoms shown, and representation of a model by Newman projections. Horizontal lines indicate the ring plane. Atoms in **1** and **2** are numbered in an analogous way.

three trimethylsilylbenzenes. Assuming additivity, we fitted the deformation parameters of $C_6H_5SiMe_3$ to the data of **1**, **2**, and **3** (see column 3 in Table 6). This gave bond angles, starting from the *ipso* angle, of 116.8, 122.2, 119.9, and 119.0°, for the monosubstituted ring. The angle distortions calculated for **1**, **2**, and **3** from additivity (column 2) agree fairly well with the experimental values (only the value for C3–C4–C5 in **2** falls outside the estimated error). The predicted *ipso* angle for $C_6H_5SiMe_3$, 116.8°, fits well with the correlation between *ipso* angles and sub-

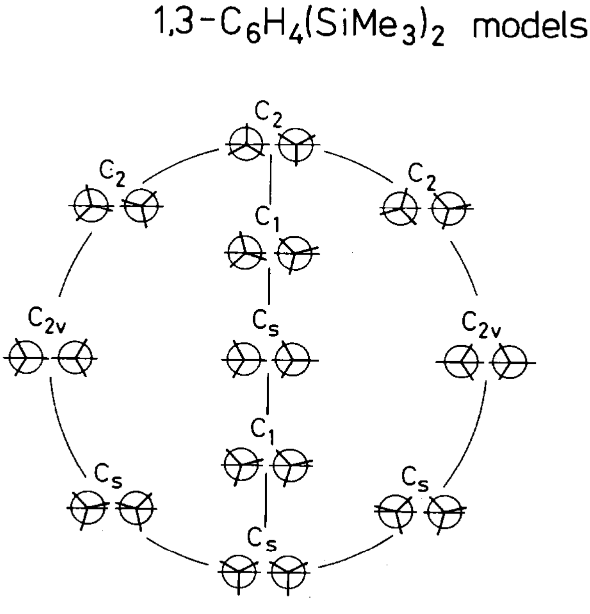

Fig. 6. The family of models of **2** with equal torsions of the $SiMe_3$ groups from their 'coplanar' positions: $\tau_3' = \tau_1'$.

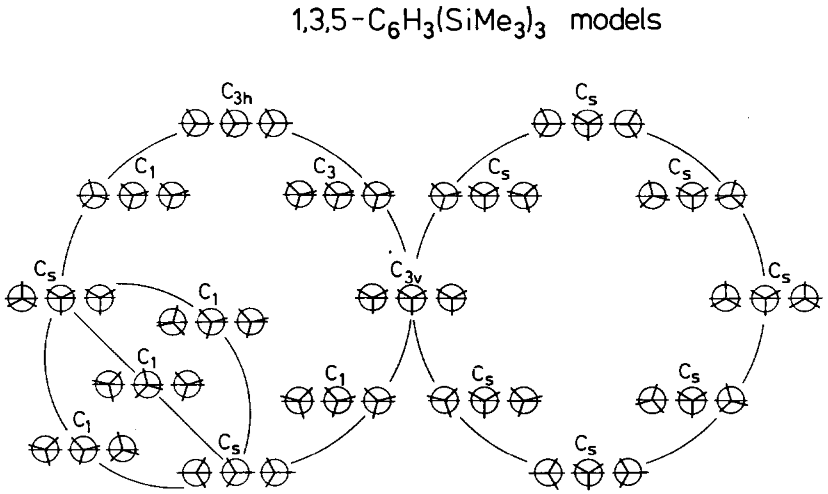

Fig. 7. The two families of models of **3**: (1) (left circle) with equal torsions of the $SiMe_3$ groups from their 'coplanar' positions: $\tau_5' = \tau_3' = \tau_1'$ and (2) (right circle) with C_s symmetry, $\tau_5' = \tau_1'$ and $\tau_3 = 90°$. The extreme left and right models are the same.

stituent electronegativities in monosubstituted benzenes (Ref. 1, Fig. 7-2, p. 284). Conversely, this observation allows an estimate of the $SiMe_3$ group electronegativity, which seems to be about the same as that of the silicon atom. The ratios of the angle deformations in $C_6H_5SiMe_3$, column 4 in Table 6, nicely parallel the ratios in column 5, which characterize the angle distortions associated with substituent electronegativity in a large series of monosubstituted benzenes (Ref. 1, p. 285, Eq. 7-1, and Ref. 22). The good agreement between columns 4 and 5 is consistent with the finding that second-row substituents, such as silicon, exert inductive effects only, and no π-electronic effects, on the ring geometry [1]. It must be emphasized, however, that such an analysis of additivity requires high-quality data (Ref. 1, p.

Table 3

Correlation matrix elements of **2** [a]

i	j	$1000\ \rho_{ij}$
Δ(SiC)	∠C6–C1–C2	−884
Δ(SiC)	l(Si1–C1)	−513
Δ(SiC)	l(C1 ··· C3)	−772
∠C6–C1–C2	l(C1 ··· C3)	851
l(C1–C2)	k_{19}	545
l(Si1–C1)	k_{19}	642
l(C1 ··· C4)	l(C1 ··· C11)	636
l(C4 ··· C11)	l(Si1 ··· H5)	535
l(C4 ··· C11)	l(Si1 ··· C32)	530
l(Si1 ··· C3)	l(C1 ··· H4)	501
l(C1 ··· H5)	l(C2 ··· C32)	525
k_{19}	k_{50}	565

[a] Only elements with $|\rho_{ij}| > 0.5$, $i \neq j$, are listed. Factors k_{19} and k_{50} scale the theoretical molecular intensities to the experimental ones in the two camera ranges 19 and 50 cm.

Table 4

Correlation matrix elements of **3** [a]

i	j	$1000\ \rho_{ij}$
Δ(SiC)	$\angle$C6–C1–C2	−807
Δ(SiC)	l(C1 ··· C3)	−608
$\angle$C6–C1–C2	l(C1 ··· C3)	730
l(Si1–C1)	k_{19}	698
l(Si1–C1)	k_{50}	509
l(C1 ··· C4)	l(C1 ··· C11)	628
l(Si1 ··· C3)	l(C1 ··· H4)	574
l(C1 ··· H2)	k_{50}	−511
l(C2 ··· H511)	l(C11 ··· C52)	649
k_{19}	k_{50}	572

[a] Only elements with $|\rho_{ij}| > 0.5$, $i \neq j$, are listed. Factors k_{19} and k_{50} scale the theoretical molecular intensities to the experimental ones in the two camera ranges 19 and 50 cm.

316), and the derived numbers in Table 6 should be treated with caution as preliminary guesses because of the relatively large experimental errors and assumptions in the determination of the angles. The consistency of the data may indicate that our assumptions were not unrealistic.

The *ipso* bond angle is 118.9 ± 0.3° in Ph_3SiH [5] and 118.2 ± 0.4° in Ph_4Si [6], *i.e.* the angular ring distortions are smaller than those in the trimethylsilylbenzenes (Table 5).

Bond lengths and angles at silicon

The mean Si–C bond lengths are well determined and are very similar in **1**, **2**, and **3**, but the bond length differences Δ(SiC) have rather large uncertainties and are correlated with other parameters. The Si–C(methyl) bonds are longer than the Si–C(aryl) bonds by some hundredths of an ångström (Table 5). A scatter diagram of Si–C bond lengths in a number of selected molecules (Fig. 8) reflects the differences in the single bond covalent radii of the carbon atom in the sp^3, sp^2,

Table 5

Geometrical parameters of trimethylsilylbenzenes [a]

	1 [b]	**2** [c]	**3** [c]
$(C–C)_{mean}$	1.408 ± 0.003	1.405 ± 0.003	1.410 ± 0.003
$(Si–C)_{mean}$	1.880 ± 0.004	1.879 ± 0.004	1.881 ± 0.004
Δ(SiC)	0.033 ± 0.007	0.018 ± 0.008	0.016 ± 0.006
Si1–C1	1.856 ± 0.007	1.866 ± 0.007	1.869 ± 0.006
Si1–C11	1.888 ± 0.004	1.884 ± 0.004	1.885 ± 0.004
C6–C1–C2	115.7 ± 0.6	116.2 ± 0.6	117.0 ± 0.6
C1–C2–C3	122.1 ± 0.3	125.0 ± 0.9	123.0 ± 0.3
C3–C4–C5		121.6 ± 0.2	
C4–C5–C6		119.5 [d]	
C1–Si–C11	109.2 ± 0.4	109.5 [d]	109.5 [d]

[a] Distances r_g are in Å, angles are in degrees. C1 is the ring *ipso* carbon atom. [b] Ref. 4, dependent r_g and angle calculated from data therein. [c] Present work. [d] Fixed parameter.

Table 6

Ring angle distortion in trimethylsilylbenzenes

Angle [a]	Distortion [b]	
	Experimental [c] (1)	From additivity [d] (2)
	1: $1,4\text{-}C_6H_4(SiMe_3)_2$	
C6–C1–C2	-4.3 ± 0.6	-4.3
C1–C2–C3	$2.1_5 \pm 0.3$	2.1_5
	2: $1,3\text{-}C_6H_4(SiMe_3)_2$	
C6–C1–C2	-3.8 ± 0.6	-3.3
C1–C2–C3	5.0 ± 0.9	4.4
C3–C4–C5	$1.5_5 \pm 0.2$	1.1_5
C4–C5–C6	-0.5 [e]	-0.1
	3: $1,3,5\text{-}C_6H_3(SiMe_3)_3$	
C6–C1–C2	-3.0 ± 0.6	-3.3
C1–C2–C3	3.0 ± 0.6	3.3

Angle [a]	Fitted to exp [f] (3)	Relative [g] (4)	Relative [h] (5)
	$C_6H_5SiMe_3$		C_6H_5X
C6–C1–C2	-3.2	1.00	1.00
C1–C2–C3	2.2	-0.68	-0.69
C2–C3–C4	-0.1	0.02	0.06
C3–C4–C5	-1.0	0.33	0.26

[a] In each molecule, C1 is the ring *ipso* carbon atom at one of the substitution positions. [b] The distortion is the deviation of the angle from 120°, *e.g* ∠(C6–C1–C2) − 120°. Angles are in degrees and are rounded off in the Table but calculations were performed to 2 decimal places or more. [c] Calculated from the angles in Table 5. [d] Calculated from the values of $C_6H_5SiMe_3$, column 3, assuming additivity. [e] Fixed parameter. [f] Fitted to the experimental data in column (1) with weights 2, 4; 2, 1, 2, 1; 3, 3 down the column. This weighting scheme corresponds to symmetry in the D_{2h}, C_{2v}, and D_{3h} rings of **1**, **2** and **3**, respectively. The condition that the sum of angle distortions in the planar hexagon must be zero was applied in the least-squares fit. [g] From column 3, related to the distortion of angle C6–C1–C2. [h] From Ref. 1, p. 285, Eq. 7-1, and Ref. 22, based on a large sample of data for various monosubstituted benzenes. This component of the distortion is associated with the electronegativity of the substituent.

and *sp* states [23], as well as steric effects in crowded or cyclic molecules, and especially the differences in ligand electronegativity, *etc*. Similar trends are observed for single bonds of carbon with other elements [24].

The silicon bond angle C1–Si–C11 obtained in **2** and **3** depended strongly on the particular conformation assumed. This parameter was therefore fixed at 109.5°. The possible tilt (θ) of the Si1–C1 bond in **2** from the external bisector of the C6–C1–C2 angle (Table 1) would be of some interest too. Parameter correlation hindered its determination for the same reasons as in the case of the C1–Si–C11 angle, and it was then fixed at 0° in the refinements [25*].

Conformation

All rotational forms which satisfy the restrictions stated above were tested in the refinements with fixed rotational angles τ_i varied in 15° steps (see Figs. 6 and 7). In spite of considerable changes in the outer regions of the theoretical radial distributions for the different models, only incomplete conclusions could be

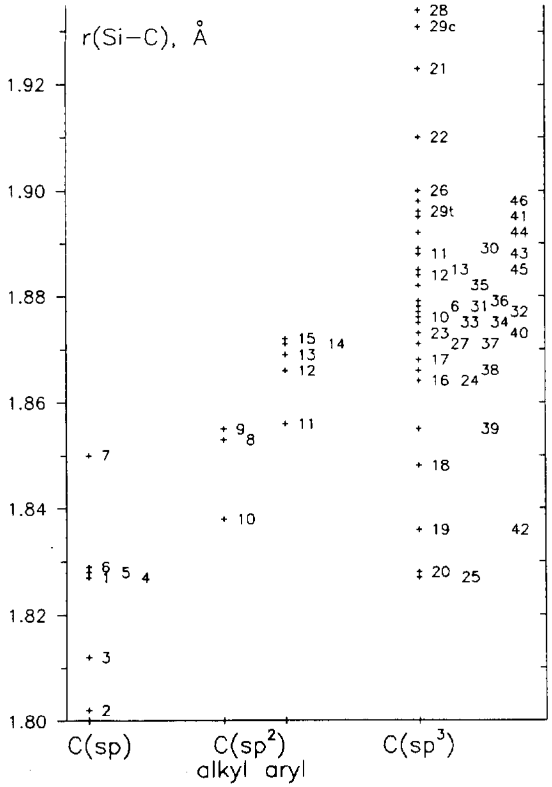

Fig. 8. Single bond lengths of silicon with *sp*, *sp*^{2}, and *sp*^{3} carbon atoms. The horizontal scale represents the carbon–carbon bond lengths in acetylene, ethene, benzene, and ethane. Data for free molecules:

1	$H_3SiC{\equiv}CH$	13	**3**	25	$F_3SiCH_2SiF_3$	35	$(Me_3Si)_3P$
2	$H_3SiC{\equiv}CCH_3$	14	$SiPh_4$	26	$Cl_3SiCCl_2SiCl_3$	36	$(Me_3Si)_3N$
3	$H_3SiC{\equiv}CCl$	15	$HSiPh_3$	27	$F_3SiCCl_2SiF_3$	37	$Me_3SiSSiMe_3$
4	$H_3SiC{\equiv}CCF_3$	16	H_3SiCH_3	28	$(Me_3C)_3SiH$	38	$Me_3SiOSiMe_3$
5	$H_3SiC{\equiv}CSiH_3$	17	$HSi(CH_3)_3$	29	$(Me_3Si)_4C$	39	$Me_3SiOOSiMe_3$
6	$Me_3SiC{\equiv}CSiMe_3$	18	$FSi(CH_3)_3$	c	Si–C(central)	40	$H_3SiCH(CH_2)_3$
7	$H_3SiC{\equiv}N$	19	$F_2Si(CH_3)_2$	t	Si–C(terminal)	41	$H_2Si(CH_2)_3$
8	$H_3SiCH{=}CH_2$	20	F_3SiCH_3	30	$(Me_3Si)_4Si$	42	$F_2Si(CH_2)_3$
9	$Si(CH{=}CH_2)_4$	21	H_3SiCF_3	31	$(H_3Si)_3CH$	43	$(H_2SiCH_2)_2$
10	$Me_2SiClCH{=}CH_2$	22	F_3SiCF_3	32	$Me_3SiSiMe_3$	44	$H_2Si(CH_2)_4$
11	**1**	23	$H_3SiCH_2SiH_3$	33	$Si(CH_3)_4$	45	$H_2Si(CH_2)_5$
12	**2**	24	$Cl_3SiCH_2SiCl_3$	34	$(H_3Si)_4C$	46	$(CH_2)_3Si(CH_2)_3$.

reached concerning the conformation. The best agreement with the experimental data was achieved for **2** with τ_i (0°, 0°), (15°, 15°), and (−15°, 15°) (the C_s and the two C_1 forms along the diameter in Fig. 6), and for **3** with (−15°, 15°, 15°) and (180°, 0°, 0°) as well as forms in its vicinity (C_1, north-west in left circle, and C_s, south in left circle, with four C_1 next to it, Fig. 7). Other forms also cannot be excluded; there is a gradual change in the goodness of fit (*R*-factor) between satisfactory and unacceptable models. Attempts to refine τ_i under the constraints given above often resulted in τ_i' (the deviation from a 'coplanar' form, see far above) from 12° to 18° but other values occurred as well. Thus, unlike that in **1**, where the angle is about 15° [4], the mean torsion of a $SiMe_3$ group related to the ring plane could not be determined in **2** and **3** (*cf.* Ref. 25*). The electron-diffraction data did not allow a distinction between free or hindered rotation about the Si–C(aryl) bonds. Connecting lines in Figs. 6 and 7 indicate relationships of conformers in principle, routes along which a model could be transferred to the neighbouring ones by small rotations. These lines should not be interpreted, however, as paths of real transitions, which probably pass through non-symmetric forms. The fact that the geometrically possible shortest C(methyl) $\cdots$ C(methyl) distance is as long as about 4.9 Å suggests that there might be no preferred mutual orientations of the $SiMe_3$ groups and also that $\theta = 0°$ (Table 1) is a reasonable assumption. Considerable steric interaction is observed, on the other hand, between large substituents in *ortho* positions [27].

It is stressed, however, that the determination of the principal geometric parameters was not hindered by the lack of conformational details of the models employed. The small uncertainties caused by the indeterminacy of the conformational choice were taken into account in the final estimation of the total errors of the parameters as described above.

Supplementary material. Tables of experimental total intensities, final backgrounds and molecular intensities, full listings of final parameters and correlation matrices, and references to sources of data in Fig. 8 are available from the authors.

Acknowledgements

We are grateful to Professor Takaaki Sonoda (Institute of Advanced Material Study, Kyushu University, Fukuoka, Japan) for suggesting this study and donating the samples, Dr. Kálmán Ujszászy (Budapest) for checking the purity of the samples, and Ms Mária Kolonits of this laboratory for experimental work. Financial support from the Hungarian Scientific Research Foundation is acknowledged (OTKA, No. 2103).

References and notes

1 A. Domenicano, in I. Hargittai and M. Hargittai (Eds.), Stereochemical Applications of Gas-Phase Electron Diffraction, Part B, VCH, New York, 1988, p. 281.
2 F.A. Keidel and S.H. Bauer, J. Chem. Phys., 25 (1956) 1218.
3 (a) L.V. Vilkov, V.S. Mastryukov and P.A. Akishin, Zh. Strukt. Khim., 5 (1964) 906; (b) L.V. Vilkov and V.S. Mastryukov, Dokl. Akad. Nauk SSSR, 162 (1965) 1306; (c) T.M. Il'enko, N.N. Veniaminov and N.V. Alekseev, Zh. Strukt. Khim., 16 (1975) 292; (d) W. Caminati and G. Cazzoli, Chem. Phys. Lett., 38 (1976) 218.
4 B. Rozsondai, B. Zelei and I. Hargittai, J. Mol. Struct., 95 (1982) 187.
5 B. Rozsondai and I. Hargittai, J. Organomet. Chem., 334 (1987) 269.
6 É. Csákvári, I.F. Shishkov, B. Rozsondai and I. Hargittai, J. Mol. Struct., 239 (1990) 291.
7 A. Domenicano, A. Vaciago and C.A. Coulson, Acta Crystallogr., Sect. B, 31 (1975) 1630.
8 (a) Y. Himeshima, H. Kobayashi and T. Sonoda, J. Am. Chem. Soc., 107 (1985) 5286; (b) H. Kobayashi and T. Sonoda, in M. Kobayashi (Ed.), Physical Organic Chemistry 1986, Elsevier, Amsterdam, 1987.
9 Y. Apeloig and D. Arad, J. Am. Chem. Soc., 107 (1985) 5285.
10 (a) B. Rozsondai, I. Hargittai and T. Sonoda, 33rd IUPAC Congress, Budapest, 1991, Book of Abstracts 2006, p. 48; (b) B. Rozsondai and I. Hargittai, 14th Austin Symposium on Molecular Structure, Austin, Texas, 1992, Abstracts.
11 T. Sonoda, personal communication, 1990.

12 I. Hargittai, J. Hernádi and M. Kolonits, Prib. Tekh. Eksp., (1972) No. 1, 239.
13 I. Hargittai, J. Hernádi, M. Kolonits and G. Schultz, Rev. Sci. Instrum., 42 (1971) 546.
14 M. Hargittai and I. Hargittai, J. Chem. Phys., 59 (1973) 2513.
15 B. Andersen, H.M. Seip, T.G. Strand and R. Stølevik, Acta Chem. Scand., 23 (1969) 3224.
16 R.A. Bonham and L. Schäfer, in J.A. Ibers and W.C. Hamilton (Eds.), International Tables for X-ray Crystallography, Vol. IV, Kynoch Press, Birmingham, 1974, Chap. 2,5.
17 (a) W. Klyne and V. Prelog, Experientia, 16 (1960) 521; (b) IUPAC Rules for the Nomenclature of Organic Chemistry, Section E: Stereochemistry, Recommendations, Pergamon Press, Oxford, 1974.
18 Angle τ_i', $i = 1, 3$, or 5, measures the smallest deviation of the $SiMe_3$ group from one of its coplanar positions: $\tau_i' = \min(\{\tau_i/60°\}, 1-\{\tau_i/60°\})\cdot 60°$, where $\{x\}$ denotes the fractional part of x, $0 \le \{x\} < 1$, *e.g.* $\{-2.75\} = 0.25$. The same τ_i' is obtained from τ_i, $\tau_i + 120°$, and $\tau_i + 240°$, and the range of τ_i' is indeed $0° \le \tau_i' \le 30°$.
19 K. Tamagawa, T. Iijima and M. Kimura, J. Mol. Struct., 30 (1976) 243.
20 R.J. Gillespie and I. Hargittai, The VSEPR Model of Molecular Geometry, Allyn and Bacon, Boston, London, 1991.
21 A. Domenicano and P. Murray-Rust, Tetrahedron Lett., (1979) 2283.
22 A. Domenicano, P. Murray-Rust and A. Vaciago, Acta Crystallogr., Sect. B, 39 (1983) 457.
23 F.A. Cotton, G. Wilkinson and P.L. Gaus, Basic Inorganic Chemistry, 2nd ed. Wiley, New York, Chichester, 1987, p. 93.
24 (a) I. Hargittai, The Structure of Volatile Sulphur Compounds, Akadémiai Kiadó, Budapest and D. Reidel, Dordrecht, 1985, p. 87; (b) B. Rozsondai and I. Hargittai, Kém. Közlem., 54 (1980) 268; (c) B. Rozsondai, B. Zelei and I. Hargittai, Magy. Kém. Foly., 88 (1982) 560.
25 Some speculation on the nature of experimental evidence and the origin of parameter correlation seems appropriate here. For the determination of the C1–Si–C11 angle, for example, the key information is expected to come from the Si1–C1 and Si1–C11 bond lengths, and nonbonded distances of the type C1 ··· C11 and C11 ··· C12. However, similar distances are correlated, and even an interchange of the latter two contributions would have no noticeable effect on the agreement between calculated and experimental radial distributions. Such difficulties in tetrahedral arrangements have been pointed out [26]. Also, longer distances that depend on this angle influence its determination, and there is an important difference between 1,4-$C_6H_4(SiMe_3)_2$ (**1**) and the 1,3- or 1,3,5-derivative (**2** or **3**) in this respect. In **1**, both C–$SiMe_3$ fragments have a common axis, so that the Si ··· C(methyl) distances are independent of the rotational form. This gives a better chance for the determination of ring distortion and individual silicon bond lengths and bond angles. In **2** and **3**, on the other hand, the Si atoms lie off the axis of the other $SiMe_3$ group(s). Thus, the presence of rotation-dependent Si ··· C(methyl) contributions in **2** and **3** has several consequences, *e.g.*, (1) they may yield more information on the mutual positions of the $SiMe_3$ groups than the C(methyl) ··· C(methyl) distances alone, (2) they conceal C(aryl) ··· C(methyl) contributions which would inform us of the mean torsion of a $SiMe_3$ group related to the ring plane, and (3) larger correlations between parameters emerge in return. The above account explains why we felt compelled to use assumed C–Si–C angles in the present analysis, and it also underlines that information on C–Si–C angles in the electron-diffraction literature should be treated with caution.
26 M. Hargittai and I. Hargittai, J. Mol. Struct., 20 (1974) 283.
27 (a) I.I. Schuster, W. Weissensteiner and K. Mislow, J. Am. Chem. Soc., 108 (1986) 6661; (b) W. Weissensteiner, I.I. Schuster, J.F. Blount and K. Mislow, J. Am. Chem. Soc., 108 (1986) 6664; (c) H. Sakurai, K. Ebata, C. Kabuto and A. Sekiguchi, J. Am. Chem. Soc., 112 (1990) 1799.